Acta Crystallographica Section D
Biological Crystallography
ISSN 0907-4449

Structures of complexes between echinomycin and duplex DNA

Jose A. Cuesta-Seijo and George M. Sheldrick*

Department of Structural Chemistry, University of Göttingen, Tammannstrasse 4, D37077 Göttingen, Germany

Correspondence e-mail: gsheldr@shelx.uni-ac.gwdg.de

Received 9 November 2004
Accepted 13 January 2005

PDB References: echinomycin–$(GCGTACGC)_2$, 1pfe, r1pfesf; 1xvk, r1xvksf; echinomycin–$(CGTACG)_2$, 1xvr, r1xvrsf; echinomycin–$(ACGTACGT)_2$, 1xvn, r1xvnsf.

The structure of the bis-intercalation complex of the depsipeptide antibiotic echinomycin with $(CGTACG)_2$ has been redetermined at a higher resolution (1.4 Å) and new high-resolution structures (1.1–1.5 Å) are reported for the complexes of echinomycin with $(GCGTACGC)_2$ (at both low and high ionic strengths) and $(ACGTACGT)_2$. The structures show the expected Hoogsteen pairing for the base pairs flanking the intercalating chromophores on the outside and Watson–Crick pairing for both base pairs enclosed by the echinomycin. In the octamer complexes but not the hexamer complex, the echinomycin molecule, which would possess a molecular twofold axis were it not for the thioacetal bridge, shows twofold disorder. In all the structures the stacking of the base pairs and chromophores is extended by intermolecular stacking. The structures provide more precise details of the hydrogen bonding and other interactions between the bis-intercalating antibiotics and the duplex DNA than were previously available.

1. Introduction

Echinomycin (Fig. 1), a depsipeptide antibiotic from *Streptomyces*, is the canonical representative of the quinoxaline antibiotics that bind to duplex DNA by bis-intercalation both *in vitro* (Waring & Wakelin, 1974; Wakelin & Waring, 1976; Waring, 1981, 1993) and *in vivo* (May *et al.*, 2004), interfering with both replication and transcription (Ward *et al.*, 1965; Sato *et al.*, 1967). These antibiotics are undergoing clinical trials as anticancer agents (Park *et al.*, 2004).

The interactions of echinomycin with DNA have been the object of extensive biological (Leslie & Fox, 2002; May *et al.*, 2004) and biochemical (Quigley *et al.*, 1986; Gallego *et al.*,

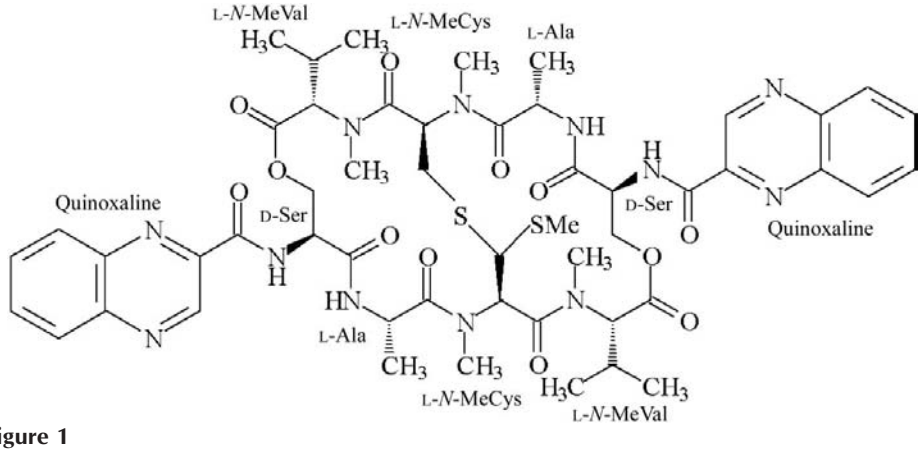

Figure 1
The echinomycin molecule. If the thioacetal bridge is ignored, the molecule possesses a twofold rotation axis.

1994) investigations. Bis-intercalation takes place preferentially around CG steps (Sayers & Waring, 1993) and has dramatic effects on the structure of the DNA. It appears to favour Hoogsteen base pairing of the bases surrounding the intercalation site (Gilbert & Feigon, 1991), with NMR studies reporting sequence and temperature-dependent behaviour (Gilbert & Feigon, 1991; Gao & Patel, 1988, 1989). It also induces unwinding of the DNA (Gilbert & Feigon, 1992). It is still not clear whether the biological activity is caused by the binding itself, by the Hoogsteen base pairing, by the unwinding or by a combination of all three.

There have been several studies of the structures of complexes of echinomycin with DNA in solution (Gilbert & Feigon, 1991, 1992; Gao & Patel, 1988, 1989) and two crystal structures have been reported of complexes of $(GCGTACGC)_2$ and $(CGTACG)_2$ with the closely related antibiotic triostin A (Wang *et al.*, 1984, 1986; Quigley *et al.*, 1986). The crystal structure of a $(CGTACG)_2$ complex with echinomycin has also been determined (Ughetto *et al.*, 1985), but unfortunately the coordinates were not published or deposited; it was stated to be very similar to the corresponding triostin A complex. The crystallizations but not the structures of tertiary actinomycin D–echinomycin–DNA and actinomycin D–triostin A–DNA have also been reported (Takusagawa & Takusagawa, 2000). Curiously, no crystal structure of echinomycin itself has been reported, although accurate structures are available for a biosynthetic derivative (echinomycin 2QN), triostin A and triostin C (Sheldrick *et al.*, 1995).

The original crystallographic studies were the first definitive observation of Hoogsteen base pairing in duplex DNA and made a seminal contribution to our understanding of the structural variability of DNA. The purpose of the current study was to take advantage of the progress of the last 20 y in crystallographic methods, especially low-temperture synchrotron data-collection and refinement techniques, to obtain precise structures of the original complex of echinomycin with $(CGTACG)_2$ as well as new echinomycin complexes with $(GCGTACGC)_2$ (at both low and high ionic strengths) and $(ACGTACGT)_2$.

Table 1
Data and refinement statistics.

Values for the highest resolution shells (or standard uncertainties in the case of the unit-cell parameters) are given in parentheses.

Crystal	GE1	GE2	CE	AE
Sequence	$(GCGTACGC)_2$	$(GCGTACGC)_2$	$(CGTACG)_2$	$(ACGTACGT)_2$
Space group	$P6_322$	$P6_322$	$C2$	$P6_322$
Unit-cell parameters				
a (Å)	39.37 (2)	39.18 (3)	29.51 (3)	39.93 (3)
b (Å)	39.37 (2)	39.18 (3)	62.62 (6)	39.93 (3)
c (Å)	79.73 (5)	79.89 (6)	34.14 (3)	80.10 (7)
β (°)			114.99 (5)	
Wavelength (Å)	0.8126	0.9000	0.9000	0.9000
Resolution (Å)	1.10 (1.20)	1.26 (1.40)	1.40 (1.50)	1.50 (1.60)
Total reflections	253373	164952	42417	139625
Unique reflections	15165	10337	10857	6499
Completeness (%)	97.2 (95.7)	99.5 (99.4)	97.8 (94.3)	99.0 (98.4)
$R_{\rm int}$ (%)	4.93 (24.25)	4.95 (35.32)	5.46 (27.5)	4.24 (42.25)
$I/\sigma(I)$	30.01 (11.47)	28.25 (6.70)	12.72 (4.87)	39.11 (9.03)
Data/restraints/parameters	15158/2074/2979	10337/5120/3121	10857/6395/4286	6499/5061/3065
R (%)	14.66	18.31	18.85	20.20
$R_{\rm free}$ (%)	16.81	22.09	23.50	23.74
PDB code	1pfe	1xvk	1xvr	1xvn

2. Materials and methods

2.1. Crystallization and data collection

Echinomycin was purchased from Sigma–Aldrich (E-4392) and used without further purification. Oligonucleotides with the self-complementary sequences GCGTACGC, ACGTACGT and CGTACG were purchased already purified by HPLC from Carl Roth GmbH and were used without further purification. Echinomycin is not water-soluble, so for crystallization it was dissolved in methanol. The DNAs were dissolved in water and the DNA and echinomycin solutions were mixed to give stock solutions containing 50% water and 50% methanol that remained clear. For the complexes with $(GCGTACGC)_2$ and $(CGTACG)_2$ a solution with 4 mg ml^{-1} DNA and a 1.05 molar ratio (DNA considered as a single strand) of echinomycin to DNA was used, while for the complex with $(ACGTACGT)_2$ the DNA concentration was 0.5 mg ml^{-1} and the molar ratio 1.1. All crystals were obtained by the hanging-drop method.

The best crystal (henceforth referred to as GE1) was obtained by mixing 2 µl of the GCGTACGC–echinomycin solution with 2 µl mother liquor consisting of 1.1 *M* Li_2SO_4, 0.05 *M* $MgCl_2$, 0.1 *M* sodium acetate buffer pH 4.5 and 0.02 *M* spermine tetrachloride. A hexagonal needle (0.85 mm long and 0.08 mm thick) grew at 293 K and was soaked for 10 s in cryoprotectant (Rubinson *et al.*, 2000) consisting of 7 *M* Li_2SO_4, 0.025 *M* $MgCl_2$ and 0.05 *M* MES buffer pH 6 before freezing. Data collection was carried out at 100 K on beamline X13 at EMBL/DESY, Hamburg. The data were integrated with *DENZO* (Otwinowski & Minor, 1997) and scaled with *SADABS* (Bruker AXS). The crystal belonged to the same space group ($P6_322$) as the crystal of the triostin A complex with the same DNA (Wang *et al.*, 1986), but the unit cell was somewhat smaller.

A second crystal (GE2) was obtained under radically different conditions from the same DNA–echinomycin stock solution by mixing 1.3 µl stock solution with 2.6 µl mother liquor containing 9% PEG 550 monomethylether, 0.05 *M* $MgCl_2$, 0.1 *M* sodium acetate buffer pH 4.5 and 0.01 *M* spermine tetrachloride. A hexagonal prism (0.2 mm in diameter and 0.1 mm thick) grew at 293 K and was frozen directly from the drop, just letting the solution in the mounting loop concentrate for 5 s by evaporation in air. Data were collected

at 100 K at the Protein Structure Factory beamline BL14.1 at BESSY using a MAR CCD detector at 100 K and integrated and scaled with *XDS* (Kabsch, 1993). The unit cell and space group were similar to those of GE1, so the starting model was taken from GE1.

1 µl of the CGTACG–echinomycin stock solution in 1:1 MeOH/H_2O was mixed with 4 µl mother liquor consisting of 30% MPD, 0.04 *M* $MgCl_2$, 0.1 *M* MES buffer pH 6 and 0.02 *M* spermine tetrachloride. A pyramidal crystal (CE) of dimensions 0.6 × 0.4 × 0.2 mm grew at 289 K and was frozen directly as it already contained sufficient cryoprotectant. Data were also collected on BL14.1 at 100 K and were integrated and scaled with *XDS*. The structure was solved by molecular replacement with *EPMR* using an edited model from GE1. Although an 'in-house' data set from a similar crystal was assigned to space group *F*222 as reported for the triostin A and echinomycin complexes with CGTACG (Wang *et al.*, 1984) and with a similar unit cell, the synchrotron data set to 1.4 Å corresponded more closely to space group *C*2, especially for the higher resolution data. R_{int} was 8.9% for *F*222 and 3.5% for *C*2. The asymmetric unit would contain one antibiotic molecule and one DNA strand in *F*222 or double this in *C*2. *C*2 was used for structure solution with *EPMR* and subsequent refinement.

A fourth crystal (AE) was obtained by mixing 20 µl ACGTACGT–echinomycin stock solution with 1 µl mother liquor containing 32% PEG 200, 6% PEG 3350, 0.05 *M* $MgCl_2$, 0.1 *M* MES buffer pH 6 and 0.02 *M* spermine tetrachloride. A bar-shaped crystal 0.6 mm long and 0.1 mm wide grew at 293 K and was frozen directly. Data were collected on BL1 at BESSY at 100 K and integrated and scaled with *XDS*. The unit cell and space group were similar to those of crystals GE1 and GE2. In all four cases the drops were equilibrated against 1 ml of the respective mother liquor containing no methanol.

2.2. Structure solution and refinement

The four structures were solved by molecular replacement using *EPMR* (Kissinger *et al.*, 1999) with the triostin A complex of $(GCGTACGC)_2$ as the initial search model and were refined using *SHELXL*-97 (Sheldrick & Schneider, 1997) with standard restraints on 1,2- and 1,3-distances (Engh & Huber, 1991; Parkinson, 1996) and restrained anisotropic displacement parameters. In all four cases the change from an isotropic model to an anisotropic model was accompanied by a substantial decrease in both *R* and R_{free} (Brünger, 1992). All four crystals showed anisotropic diffraction as a result of extended base stacking, but this

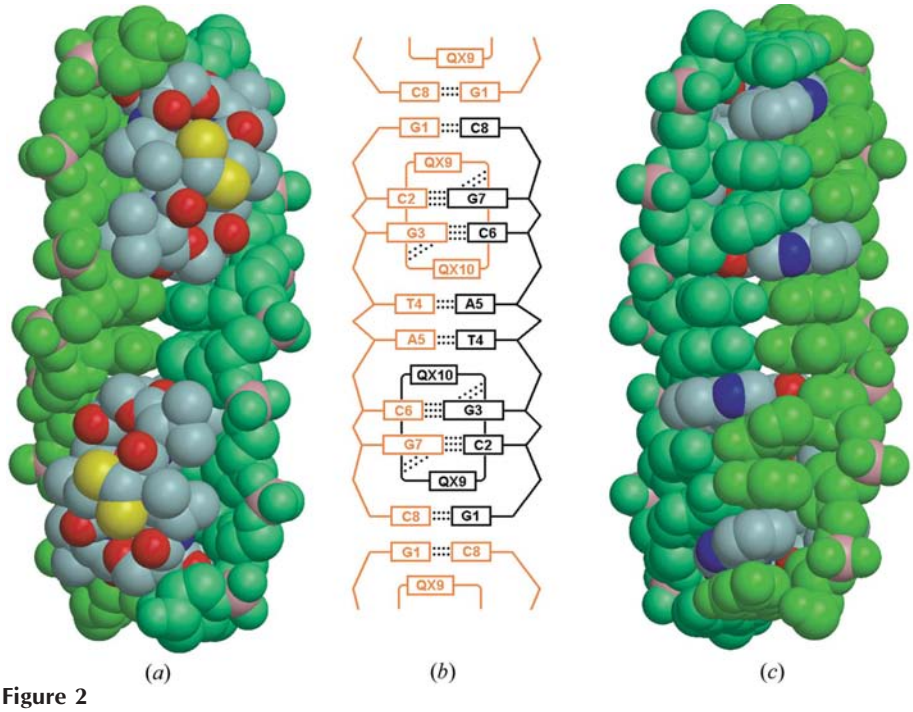

Figure 2
The echinomycin $(GCGTACGC)_2$ complex GE1 (*a*) showing the protruding thioacetal bridges, (*b*) diagrammatic representation of the base and chromophore stacking showing also the stacking to symmetry-equivalent molecules (the asymmetric unit is shown in black) and (*c*) rotated 180° from (*a*) showing the chromophores.

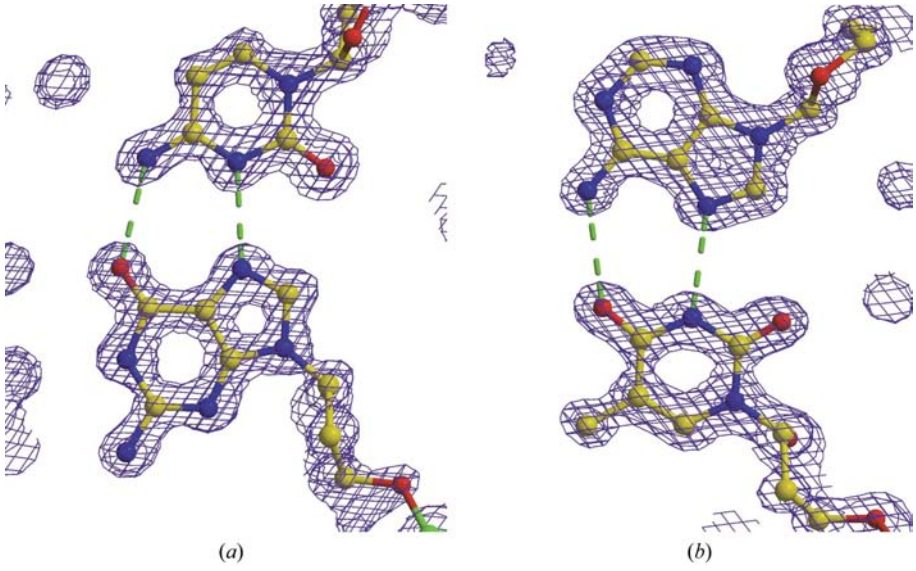

Figure 3
$2F_o - F_c$ maps at the 2σ level of (*a*) the G1–C8 and (*b*) the T4–A5 Hoogsteen base pairs in structure GE1.

appears to have been modelled adequately by the anisotropic refinement. The final data and refinement statistics are given in Table 1.

3. Results and discussion

3.1. The $P6_322$ structures

All three octamer complexes display nearly identical bis-intercalation geometry, with an asymmetric unit consisting of one DNA strand and one echinomycin molecule. A crystallographic twofold axis generates the duplex, with two echinomycin molecules intercalating around both CG steps (Fig. 2). The echinomycin molecules lie in the minor groove, with the quinoxalines protruding into the major groove. All four G–C and A–T base pairs on the outside of the intercalation sites are Hoogsteen base-paired with the purines rotated to the *syn* orientation relative to the sugars (Fig. 3), while all four G–C base pairs within the intercalation sites are in the standard Watson–Crick configuration. The hydrogen-bonding distances for the base pairing are listed in Table 2.

The antibiotics interact with the DNA not only by intercalation and a great number of van der Waals contacts but also by four hydrogen bonds between the carbonyl groups of Ala12 and Ala17 to N2 of G7 and G3, respectively, and between the amide N atoms of Ala12 and Ala17 to N3 of G7 and G3, respectively (Table 3). This is in contrast to the results of Wang *et al.* (1986) for the octamer complex with triostin A, where one of these contacts was 3.86 Å. The AE crystal exhibited extensive disorder in the terminal base pairs at both the 5′ and 3′ ends, so two conformations were modelled for the bases involved and for the corresponding sugars. Hoogsteen base pairing is preserved with similar geometry in both cases and the disordered conformations possess similar occupancies and displacement parameters. The disordered base pairs stack on one side with their symmetry equivalents (also disordered) and on the other with a quinoxaline that shows no disorder and interacts most strongly with the adenine in both disordered components.

The duplexes form infinite columns along the *c* axis of the crystals, with the terminal bases stacking on their symmetry equivalents. Two kinds of solvent channels are formed along *c*, with diameters of approximately 30 and 10 Å. The thioacetal bridges of echinomycin face the large channels, while the phosphates of the DNA backbone face the small channels. Octahedrally coordinated magnesium ions link the phosphates of G4 from different columns together in the small solvent channels of GE2 and AE but are not observed in GE1; we suspect that they have been replaced by less ordered Li^+ cations in GE1. There are also intermolecular interactions between both terminal nucleobases at the 5′ end of the DNA and both terminal phosphates at the 3′ end.

3.2. The *C*2 structure

The asymmetric unit of the hexamer complex consists of a duplex DNA with echinomycin molecules bis-intercalating around both CG steps. Both central A–T base pairs are again

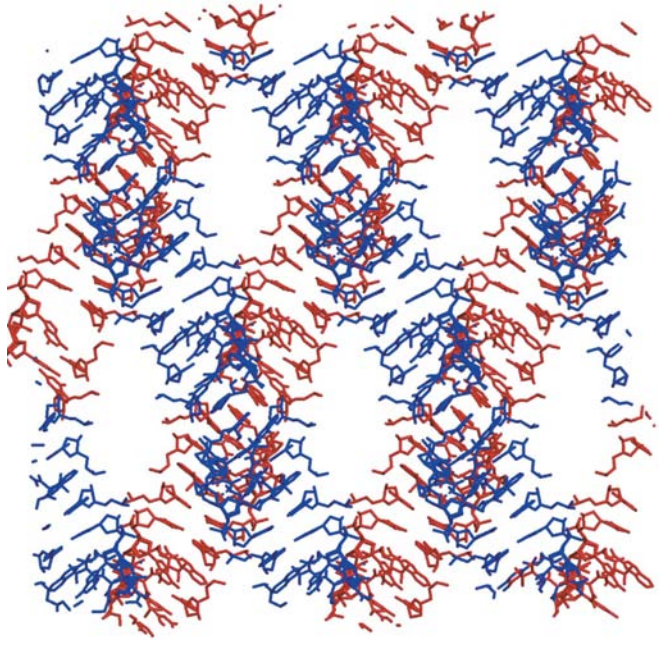

Figure 4
The criss-crossed columns of stacked bases and chromophores in the *C*2 structure.

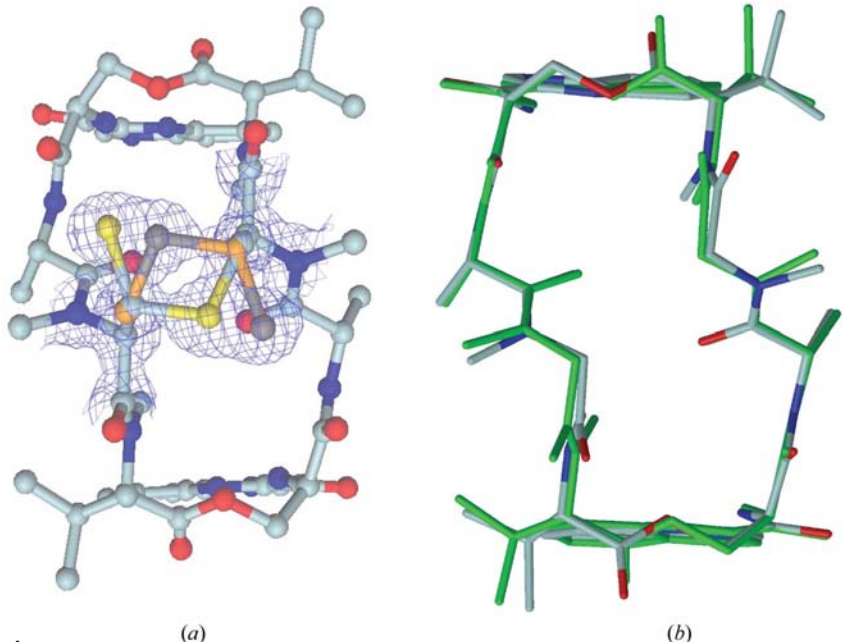

Figure 5
(*a*) The thioacetal bridge in the structure GE1 showing the twofold disorder ($2F_o - F_c$ map contoured at 1σ); (*b*) a superposition of the (not disordered) echinomycin molecule in the *C*2 structure on itself after rotation of 180° about the molecular pseudo-twofold axis.

Table 2
Hydrogen-bonding distances in the base pairs.

For GE1, GE2 and AE, 100 has been added to the residue numbers of symmetry-equivalent bases. W-C stands for Watson–Crick and HG for Hoogsteen base pairing. For AE both conformations for the first base pair are included.

	Distances (Å)				Distances (Å)	
Atoms	GE1	GE2	CE	Atoms	AE	Base-pair type
G1 O6···C108 N4	2.85	2.85	—	A1 N6···T108 O4	2.92/2.89	HG
G1 N7···C108 N3	2.73	2.68	—	A1 N7···T108 N3	2.77/2.86	
C2 O2···G107 N2	2.84	2.77	2.80	C2 O2···G107 N2	2.86	W-C
C2 N3···G107 N1	2.89	2.87	2.88	C2 N3···G107 N1	2.92	
C2 N4···G107 O6	2.86	2.77	2.83	C2 N4···G107 O6	2.82	
G3 N1···C106 N3	2.93	2.90	2.94	G3 N1···C106 N3	2.84	W-C
G3 N2···C106 O2	2.80	2.77	2.83	G3 N2···C106 O2	2.76	
G3 O6···C106 N4	2.97	2.86	2.87	G3 O6···C106 N4	2.93	
T4 N3···A105 N7	2.85	2.86	2.89	T4 N3···A105 N7	2.85	HG
T4 O4···A105 N6	2.95	2.78	2.90	T4 O4···A105 N6	2.89	
A5 N6···T104 O4	2.95	2.78	2.94	A5 N6···T104 O4	2.89	HG
A5 N7···T104 N3	2.85	2.86	2.79	A5 N7···T104 N3	2.85	
C6 O2···G103 N2	2.80	2.77	2.78	C6 O2···G103 N2	2.76	W-C
C6 N3···G103 N1	2.93	2.90	2.95	C6 N3···G103 N1	2.84	
C6 N4···G103 O6	2.97	2.86	2.98	C6 N4···G103 O6	2.93	
G7 N1···C102 N3	2.89	2.87	2.84	G7 N1···C102 N3	2.92	W-C
G7 N2···C102 O2	2.84	2.77	2.84	G7 N2···C102 O2	2.86	
G7 O6···C102 N4	2.86	2.77	2.83	G7 O6···C102 N4	2.82	
C8 N4···G101 O6	2.85	2.85	—	T8 N3···A101 N7	2.77/2.86	HG
C8 N3···G101 N7	2.73	2.68	—	T8 O4···A101 N6	2.92/2.89	

Table 3
Hydrogen-bond lengths between the echinomycins and the DNAs.

Notation as in Table 2.

Crystal	Donor	Acceptor	Distance (A)
GE1	Ala12 N	G7 N3	3.05
GE2	Ala12 N	G7 N3	3.03
AE	Ala12 N	G7 N3	3.12
CE	Ala12 N	G3 N3	2.95
CE	Ala112 N	G103 N3	2.99
GE1	Ala17 N	G3 N3	3.09
GE2	Ala17 N	G3 N3	3.01
AE	Ala17 N	G3 N3	2.93
CE	Ala17 N	G107 N3	2.98
CE	Ala117 N	G7 N3	2.96
GE1	G7 N2	Ala12 O	3.13
GE2	G7 N2	Ala12 O	3.22
AE	G7 N2	Ala12 O	3.16
CE	G3 N2	Ala12 O	3.18
CE	G103 N2	Ala112 O	3.15
GE1	G3 N2	Ala17 O	3.16
GE2	G3 N2	Ala17 O	3.08
AE	G3 N2	Ala17 O	3.19
CE	G107 N2	Ala17 O	3.14
CE	G7 N2	Ala117 O	3.17

in the Hoogsteen configuration and all four G–C pairs show Watson–Crick pairing, so the structure resembles that of the octamer complex with the terminal base pairs removed. The duplexes again stack to form infinite columns, but this time with quinoxaline–quinoxaline stacking. There are two families of columns crossing each other at an angle (Fig. 4). The crystal is held together by van der Waals contacts between the different colums in which the thioacetals also participate and by magnesium ions bridging guanine N3 and quinoxaline N9 of different complexes.

In the *F*222 superstructure the asymmetric unit has only one strand of DNA and one echinomycin molecule, with the second pair generated by a crystallographic twofold axis that is not present in the *C*2 model. This twofold axis appears to be violated mainly by the first two nucleotides of each strand and by the solvent model, though even in *C*2 it was necessary to model alternative conformations for their sugars and phosphates. The r.m.s.d. for the other 14 residues (four in DNA, ten in echinomycin) is 0.11 Å after superimposing both chains with *XFIT* (McRee, 1999); for all 16 residues it is 0.82 Å. The *F*222 superstructure appears to be similar to that reported by Ughetto *et al.* (1985) for the triostin A and echinomycin complexes with $(CGTACG)_2$, but whereas we again find all four hydrogen bonds between the alanines and the guanines (Table 3), Ughetto *et al.* (1985) reported distances of 3.6 Å for the echinomycin complex and 4.1 Å for the triostin A complex for one of these hydrogen bonds.

3.3. Twofold echinomycin disorder

Echinomycin possesses a cyclic depsipeptide backbone, made more rigid by the thioacetal bridge, and two chromophores that can orientate themselves approximately perpendicular to the peptide ring for bis-intercalation. The thioacetal bridge between N-methyl-cysteines breaks the twofold symmetry of the molecule. In the biosynthetic precursor triostin A there is a disulfide instead of thioacetal bridge, so the twofold molecular symmetry is in principle preserved, although the molecule deviates somewhat from twofold symmetry in the crystal (Sheldrick *et al.*, 1995). In the $P6_322$ structures the antibiotic is disordered by a twofold rotation; since the cyclopeptide ring atoms scarcely deviate from the twofold molecular symmetry, we were able to model the antibiotic with alternative conformations (Fig. 5*a*) for the thioacetal bridge and full occupancies for the remaining atoms. The occupancies of the thioacetal bridge conformations refined to 56/44% (GE1), 51/49% (GE2) and 54/46% (AE). There was no difference density corresponding to the S-methyl groups in GE1 and AE, so they were omitted from the final model in these structures.

This twofold disorder was not seen in the *C*2 structure. We attribute this conformational selection to crystal contacts between the thioacetal bridges of symmetry-equivalent molecules; these are absent in the $P6_322$ structure, where the thioacetals border the solvent channels. A superposition of the echinomycins in the *C*2 structure on themselves after a 180°

rotation gave r.m.s. deviations of 0.20 Å between the backbone atoms and chromophores (Fig. 5*b*).

3.4. Overall structures of the complexes

A comparison of all four structures shows that they adopt basically the same structure. Despite different crystallization conditions and morphology, the crystals GE1 and GE2, which involved the same DNA sequence, are similar, with a mean deviation of 0.60 Å for all atoms. The r.m.s. deviation between GE1 (the highest resolution structure) and AE is 0.83 Å and between the common atoms of GE1 and CE it is 1.36 Å, with the biggest differences being concentrated in the thioacetal bridges and the quinoxalines, which are involved in crystal contacts in CE.

3.5. Base pairing and stacking

For a CG base pair to adopt the Hoogsteen conformation the cytosine has to be protonated at N3. The pK_a of cytosine is 4.6 (Windholz, 1983). The crystals GE1 and GE2 grew at pH 4.5, but the cryoprotection will have changed this to pH 6 for GE1; we observed that crystals also grew at pH 6, as observed by Quigley *et al.* (1986), but did not at pH 7. In spite of the high-resolution data, no clear electron density was observed for this hydrogen in the $F_o - F_c$ maps, so it was not included in the models.

The stacking of the base pairs with each other and with the quinoxalines is a defining feature of the structures. When just the DNA bases and quinoxalines of GE1 are superimposed on the triostin A complex of Wang *et al.* (1986) the r.m.s. deviation is 0.50 Å (Fig. 6), but the conformations of the sugars 3, 6 and 7 differ appreciably. In the echinomycin structures they lie closer to the plane of the bases than in the triostin A complex, with χ angles in the B-DNA range (around -108°). The superposition of the base pairs of the hexamer complex of triostin A (Wang *et al.*, 1984) against those of the two complexes in the asymmetric unit of CE gives an almost perfect fit, with r.m.s. deviations of 0.18 and 0.17 Å; the sugars also superimpose well in these fits.

In the four structures reported here, the CG base pairs inside the intercalation sites are appreciably buckled and are involved in some close contacts; the interactions between the β C atoms of the alanines in the echinomycins with the sugars of these nucleotides may well be responsible for this buckling. The chromophores do not show any buckling. The stacking overlap of the quinoxaline groups is always substantial relative to the purine bases external to the bis-intercalation sites (and to other quinoxalines in crystal contacts in CE) but much smaller relative to the internal bases, even when the carbonyl group of the quinoxalines is included.

4. Conclusions

The overall structures of the complexes are similar to those reported for the triostin A complexes of $(GCGTACGC)_2$ and $(CGTACG)_2$ and (as far as can be judged without the coordinates) the echinomycin complex of $(CGTACG)_2$ (Wang *et al.*, 1984, 1986; Ughetto *et al.*, 1985; Quigley *et al.*, 1986). The structures are characterized by bis-intercalation of echinomycin around all CG steps, either terminal or internal to the DNA duplex. The bases flanking the bis-intercalation sites show Hoogsteen pairing, whereas the bases enclosed by the echinomycin show Watson–Crick pairing. The stacking is extended by intermolecular interactions between base pairs in the octamer complexes and between chromophores in the hexamer structure. This intermolecular stacking imposes some rigidity on the structures; an isolated complex in solution might be expected to show more flexibility in the mode of base pairing *etc.*, as indeed indicated by the NMR studies.

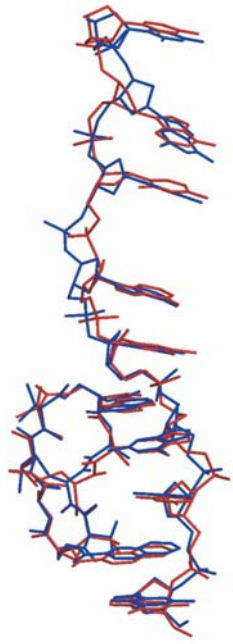

Figure 6
A comparison of GE1 (blue) with the triostin A $(GCGTACGC)_2$ complex (red) (Wang *et al.*, 1986).

The echinomycin molecule possesses a pseudo-twofold symmetry axis that is violated significantly only by the thioacetal bridge; this leads to twofold disorder of the bis-intercalating antibiotic in the octamer complexes but not in the hexamer complex, where intermolecular close contacts between thioacetals lead to selection of a single echinomycin orientation. There are no interactions between the thioacetal bridges and DNA.

There are significant differences in detail, for example the hydrogen-bond patterns, sugar conformations and buckling of the base-pairs, when the new structure determinations are compared with the structures determined in the mid-1980s. These must at least in part be attributed to the difficulties of refining such complex structures adequately in those days and indeed the original authors urged caution in the interpretation of such details for this reason.

We should particularly like to thank Michael J. Waring and Ulf Diederichsen for arousing our interest in this subject and for many discussions, Ehmke Pohl and Ilka Müller for assis-

tance at the beamline and Isabel Usón for help with the refinements. We are grateful to the Fonds der Chemischen Industrie, the Deutsche Forschungsgemeinschaft (SFB416) and the European Community (Access to Research Infrastructure Action of the Improving Human Potential Programme to the EMBL Hamburg Outstation, contract No. HPRI-1999-CT-000017) for support and to EMBL/DESY, Hamburg and BESSY, Berlin for generous allocations of beamtime.

References

Brünger, A. T. (1992). *Nature (London)*, **355**, 472–475.
Engh, R. A. & Huber, R. (1991). *Acta Cryst.* A**47**, 392–400.
Gallego, J., Luque, F. J., Orozco, M., Burgos, C., Alvarez-Builla, J., Rodrigo, M. M. & Gago, F. (1994). *J. Med. Chem.* **37**, 1602–1609.
Gao, X. & Patel, D. J. (1988). *Biochemistry*, **27**, 1744–1751.
Gao, X. & Patel, D. J. (1989). *Quart. Rev. Biophys.* **22**, 93–138.
Gilbert, D. E. & Feigon, J. (1991). *Biochemistry*, **30**, 2483–2494.
Gilbert, D. E. & Feigon, J. (1992). *Nucleic Acids Res.* **20**, 2411–2420.
Kabsch, W. (1993). *J. Appl. Cryst.* **26**, 795–800.
Kissinger, C. R., Gehlhaar, D. K. & Fogel, D. B. (1999). *Acta Cryst.* D**55**, 484–491.
Leslie, K. D. & Fox, K. R. (2002). *Biochemistry*, **41**, 3484–3497.
McRee, D. (1999). *J. Struct. Biol.* **125**, 156–165.
May, L. G., Madine, M. A. & Waring, M. J. (2004). *Nucleic Acids Res.* **32**, 65–72.
Otwinowski, Z. & Minor, W. (1997). *Methods Enzymol.* **276**, 307–326.
Park, J. Y., Park, S. J., Shim, K. Y., Lee, K. J., Kim, Y.-B., Kim, Y. H. & Kim, S. K. (2004). *Pharm. Res.* **50**, 201–207.
Parkinson, G. (1996). *Acta Cryst.* D**52**, 57–64.
Quigley, G. J., Ughetto, G., van der Marel, G. A., van Boom, J. H., Wang, A. H.-J. & Rich, A. (1986). *Science*, **232**, 1255–1258.
Rubinson, K. A., Ladner, J. E., Tordova, M. & Gilliland, G. L. (2000). *Acta Cryst.* D**56**, 996–1001.
Sato, K., Shiratori, O. & Katagiri, K. J. (1967). *J. Antibiot.* **20**, 270–276.
Sayers, E. W. & Waring, M. J. (1993). *Biochemistry*, **32**, 9094–9107.
Sheldrick, G. M., Heine, A., Schmidt-Bäse, K., Pohl, E., Jones, P. G., Paulus, E. & Waring, M. J. (1995). *Acta Cryst.* B**51**, 987–999.
Sheldrick, G. M. & Schneider, T. R. (1997). *Methods Enzymol.* **277**, 319–343.
Takusagawa, H. L. & Takusagawa, F. (2000). *Acta Cryst.* D**56**, 344–347.
Ughetto, G., Wang, A. H.-J., Quigley, G. J., van der Marel, G. A., van Boom, J. H. & Rich, A. (1985). *Nucleic Acids Res.* **13**, 2305–2323.
Wakelin, S. P. & Waring, M. J. (1976). *Biochem. J.* **157**, 721–740.
Wang, A. H.-J., Ughetto, G., Quigley, G. J., Hakoshima, T., van der Marel, G. A., van Boom, J. H. & Rich, A. (1984). *Science*, **225**, 1115–1121.
Wang, A. H.-J., Ughetto, G., Quigley, G. J. & Rich, A. (1986). *J. Biomol. Struct. Dyn.* **4**, 319–342.
Ward, D. C., Reich, E. & Goldberg, I. H. (1965). *Science*, **149**, 1259–1263.
Waring, M. J. (1981). *Ann. Rev. Biochem.* **50**, 159–192.
Waring, M. J. (1993). *Molecular Aspects of Anticancer Drug–DNA Interactions*, edited by S. Neidle & M. J. Waring, Vol. 1, pp. 213–242. London: Macmillan.
Waring, M. J. & Wakelin, L. P. G. (1974). *Nature (London)*, **252**, 653–657.
Windholz, M. (1983). Editor. *The Merck Index*, 10th ed. Rahway, NJ, USA: Merck & Co. Inc.